FRACTURE BEHAVIOUR OF WELD JOINTS MADE OF PEARLITIC AND BAINITIC STEEL

Libor Válka[1,*], Ivo Dlouhý[1]

[1] Institute of Materials Science and Engineering, NETME centre, Faculty of Mechanical Engineering, Brno University of Technology, Technická 2, 616 69 Brno, Czech Republic

[*]corresponding author: Tel.: +420 541143172, e-mail: valka@fme.vutbr.cz

Resume

The paper is concerned with microstructure evaluations and the hardness and fracture behaviour of welded joints made from cast bainitic Lo8CrNiMo steel and pearlitic rail steel of the type UIC 900A. The materials mentioned are predetermined for frogs of switches. The study is based mainly on microstructural observations and hardness measurements of the base materials, weld, and heat affected zone (HAZ). Dynamic fracture toughness was evaluated based on data from pre-cracked Charpy type specimens. The pearlitic UIC 900A steel and its HAZ had the lowest dynamic fracture toughness values and therefore the highest risk of brittle fracture. At application temperature range, this steel is on the lower shelf of the ductile-to-brittle transition, and the tempering in the HAZ did not affect the toughness substantially. The cast bainitic steel in the weld joint is characterized by higher toughness values compared to the pearlitic one, and a further increase in toughness may be expected in the HAZ. The weld zone itself is characterized by high scatter of toughness data; nevertheless, all the values are above the scatter band characterizing the pearlitic steel.

Available online: http://fstroj.uniza.sk/journal-mi/PDF/2016/05-2016.pdf

Article info

Article history:
Received 15 March 2016
Accepted 25 April 2016
Online 12 June 2016

Keywords:
Welded joint;
Bainitic steel;
Pearlitic steel;
Dynamic fracture toughness;
Point crossing frog.

ISSN 1335-0803 (print version)
ISSN 1338-6174 (online version)

1. Introduction

The current stage of advances in rail transport can be characterized by increasing speed, growth of axle load and transported volume, and the requirement to extend the rails' operating lifetime. In consequence of this trend, the demands regarding the quality of rail materials and the search for new designs and material solutions are increasing significantly [1–3]. One of the most important and most stressed part of the track superstructure is the frog. According to the structural solutions of crossings, frogs can be categorized as: (i) built-up, where the parts are manufactured from flat-bottom rails or special frog profiles, respectively; (ii) mounted-monolithic, consisting of certain compact units (weldments); and (iii) a monoblock, where a frog and connecting rails are designed as a compact block; that is, four rails are welded to the cast frog. Welding is done mostly by flash welding technology [4].

Austenitic manganese steel UIC 866 is a well-known material that is still used for the manufacture of cast frogs. This steel can be strengthened by cold forming and retains excellent toughness at very low temperatures. The disadvantage of this steel is its production cost and difficult machining, especially its problematic surfacing and welding with conventional rail materials. Compared with austenitic steel, the low-carbon bainitic alloy steel Lo8CrNiMo presents an advantageous combination of material and process parameters [5, 6]. This steel has been extensively studied and it has been shown that the key parameters surpass those of manganese austenitic steel UIC 866 in many cases. One of these key features is the dynamic fracture toughness, which represents the resistance of the material to fracture under dynamic loading conditions [6].

Therefore, within the complex study of cast bainitic crossings, the fracture behaviour of weld

with pearlitic rail steel was evaluated. The weld hides a number of pitfalls from the microstructural point of view, including negative impacts on the fracture behaviour. On the other hand, however, it could open the way for use in monoblock crossings. The study also includes in-service bending tests [7] and the evaluation of fractures in welds of pearlite and bainitic rails, but it cannot be done without an analysis of the impact of potentially negative structures on the dynamic fracture toughness.

The aim of this study was to determine the risks associated with welding of bainitic and pearlite steels and whether the weld joint reduces the overall resistance to brittle fracture under dynamic loading.

2. Materials, test specimens, and experimental procedures

Bainitic cast (Lo8CrNiMo [1]) and standard pearlitic rail UIC grade 900A steels with the chemical composition shown in Table 1 were used as the test materials.

Type UIC 60 rails with a length of approximately 0.75 m were cast from the bainitic Lo8CrNiMo steel and were subsequently annealed by slow heating to the austenitizing temperature of 900 - 920 °C, cooled by compressed air, and tempered at 260 - 280 °C. The dwell time (four hours) at austenitizing temperature guarantees the desired austenite homogeneity. Cooling by compressed air follows the achievement of such a cooling rate, which provides the higher hardness and strength required for rail profile materials, mainly for crossing frogs. A tempering temperature of 260 - 280 °C ensures the reduction of internal stresses. This method of heat treatment resulted in the mainly bainitic structure of Lo8CrNiMo steel.

Lo8CrNiMo steel castings were welded by flash welding technology ("butt") with standard rail steel type UIC 60 of grade UIC 900A, which also had a length of ca. 750 mm. The welding was carried out on a computer-controlled Schlatter GAA 100/580 resistance welding machine in DT Výhybkárna a mostárna, s.r.o. Prostějov. The total loss of both materials after flash welding and squeezing was on average 29.3 mm, and the length loss of the Lo8CrNiMo steel was about 13 mm. The results presented in this paper represent data obtained from four weldments.

To determine the exact positions of the specimens relative to the position of the weld axis, a detailed analysis of a part length of 120 mm (120×172×12 mm) cut out from one of the weldments was made. Besides etching on the macrostructure, measurements of hardness were taken over the entire surface. A detailed metallographic analysis and hardness HV10 measurements were then carried out on strips cut off from the head and base of the plate.

Based on the results obtained from the plate, the exact positions of the test specimens taken from other weldments were determined. The fracture behaviour of both base materials (i.e. bainitic cast iron and pearlitic rail steel) was monitored, as well as the fracture behaviour in the heat affected zone (HAZ) in the location of the highest brittleness of these materials and in the axis of the weld. The most brittle place was considered to be the part of the HAZ at which the highest hardness was measured. To determine the dynamic fracture toughness, the Charpy-type test specimens with fatigue cracking [referred to as "pre-cracked Charpy" (PC)] were manufactured from the abovementioned parts of the rails. The fatigue crack was oriented perpendicular to the rail head surface and the fracture spread inwards in the rail. Dynamic loading was carried out on an instrumented impact tester according to the ESIS standard [8]. Tests were conducted at temperatures from –60 to +80 °C, and the impact velocity was within the range of 1.0 - 1.4 $m.s^{-1}$ (i.e. low blow testing). Procedures of fracture toughness determination based on the relevant standards are described in [7, 9].

Table 1

Chemical composition of Lo8CrNiMo bainitic steel and UIC 900A pearlitic rail steel (in wt. %).

	C	Si	Mn	P	S	N
Lo8CrNiMo	0.11-0.15	max 0.5	0.5-0.8	max 0.015	max 0.012	max 0.012
900A	0.6-0.8	0.1-0.5	0.8-1.3	max 0.04	max 0.04	-
	Cr	**Ni**	**Mo**	**Al**	**Ti**	**V**
Lo8CrNiMo	1.6-2.0	2.6-3.0	0.4-0.5	max 0.045	0.05	max 0.13
900A	-	-	-	-	-	-

3. Experimental results and discussion

3.1 Hardness and microstructural analysis

To get an idea about the size and shape of the HAZ and to determine the location and course of the weld axis, etching of the macrostructure of the plate cut out in the longitudinal direction in the axial plane of the rail was performed. Oberhoffer and Whiteley etchants were used for etching, respectively. The shape of the HAZ fits the rail profile; that is, the HAZ width of the head and foot of the rail is wider than the HAZ width of the web, whereas the HAZ of the bainitic steel is wider than the HAZ of the pearlitic steel (43 mm compared with 29 mm). The axial plane of the weld is clearly visible in Fig. 1a. An apparent difference between the rolled pearlitic structure with the fibres deformed near the weld axis as a result of squeezing and the dendritic structure of Lo8CrNiMo steel is clearly visible. It is apparent from Fig. 1a that the weld is not an ideal plane because of the larger plastic deformation of the bottom half of the UIC 900A rail at the moment of weld creation.

For the mapping of properties in the weld area, HAZ, and base material, hardness measurements were performed on the surface of the plate. The hardness HRC was measured in the direction perpendicular to the plane of the weld with a puncture distance of 10 mm. The distance between rows of stitches was 10 mm in the head and foot parts of the plate and 20 mm in the web. The progress of hardness in the head, web, and base parts of the rail is shown in Fig. 1b, c, d.

For verification and possible refinements of hardness behaviour in relation to microstructure, the Vickers hardness was evaluated in the same direction. Hardness HV10 was measured on strips 25 mm in width cut off from the head and base of the plate with a step of 5 mm from the plate edge (see Fig. 2a, b). Two rows of stitches were measured in the strip of the head part, one of them closer to the top of rail, the second closer to the centre of the head rail. The positions of the maximum hardness values were established based on the hardness behaviour and served as the starting points for the positioning of the PC test specimens.

In the area of local overheating in the vicinity of the weld axis on the side of the UIC 900A rail, the metallographic analysis (Fig. 3a) showed a coarsening of the ferrite-pearlite structure, with ferrite excluded on the pearlitic grains boundaries. A Widmanstätten morphology was observed in some cases. A lamellar pearlitic structure of grain size 3 - 4 according to the ČSN 42 0462 standard [10] was apparent in the pearlite. In the direction of the UIC 900A base material, the structure became a fine-grained pearlitic structure with a smaller portion of ferrite. The pearlitic structure with occasional occurrence of structurally separated ferrite also occurred in the area of maximum hardness (about 17 mm from the weld axis; see Fig. 3b). The structure away from that point towards the base material is almost purely pearlitic.

In the area of local overheating of the Lo8CrNiMo steel, a bainitic structure with coarse bainitic ferrite laths was apparent. Similarly, in the HAZ, the structure of Lo8CrNiMo steel consisted of morphologically rough bainitic ferrite with carbides. The same conclusion applies to sites with the maximum hardness (about 24 mm from the weld axis; see

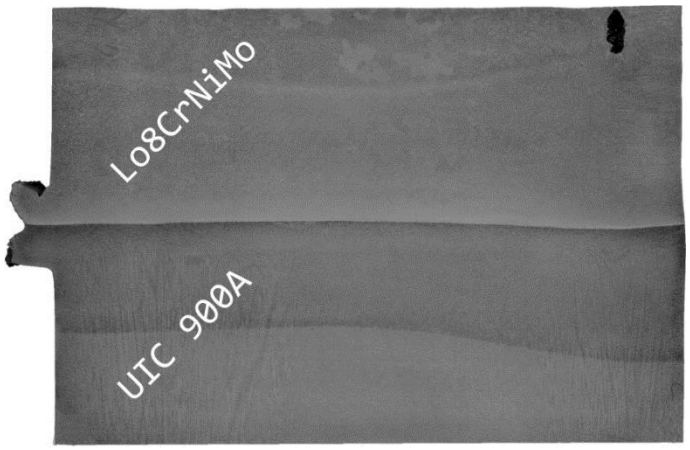

a) macrostructure of the heat affected zone near to the weld joint of UIC 900A and Lo8CrNiMo steels

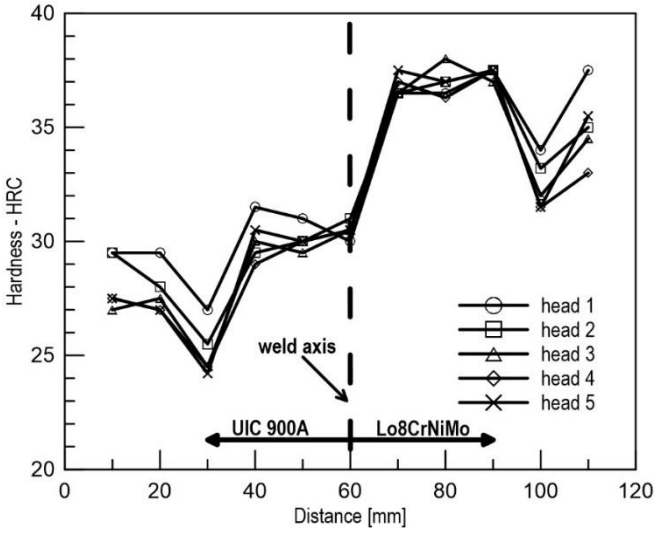

b) progress of hardness in the head part of the weld

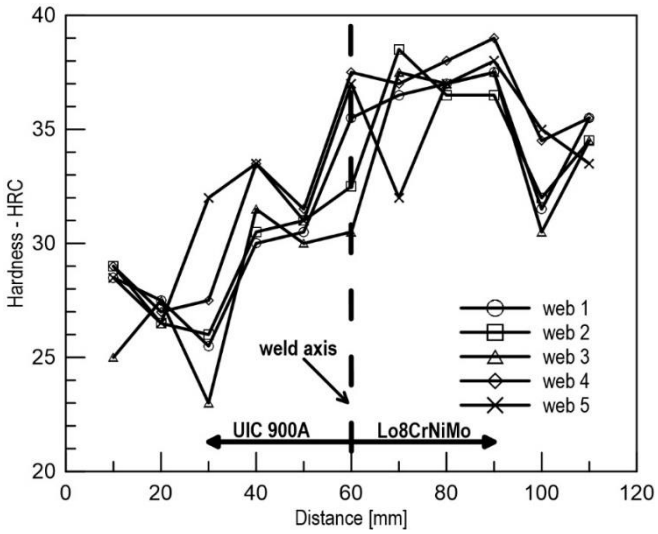

c) progress of hardness in the web part of the weld

Fig. 1. Macrostructure of the heat affected zone near to the weld joint of UIC 900A and Lo8CrNiMo steels and the progress of hardness.

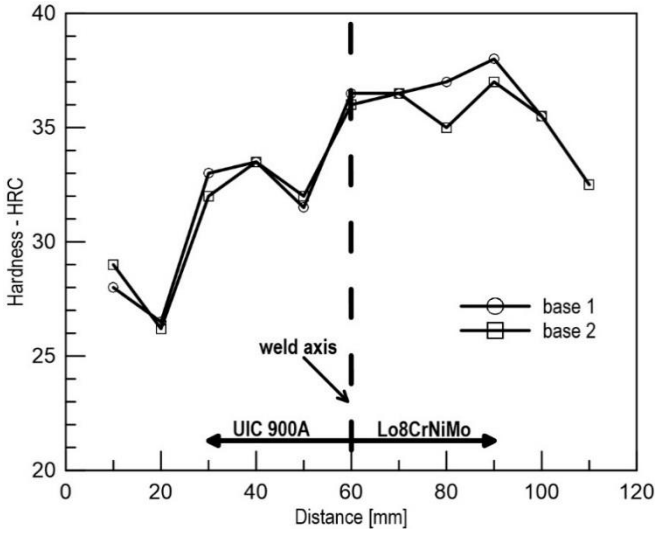

d) progress of hardness in the base part of the weld

Continuing of Fig. 1. Macrostructure of the heat affected zone near to the weld joint of UIC 900A and Lo8CrNiMo steels and the progress of hardness.

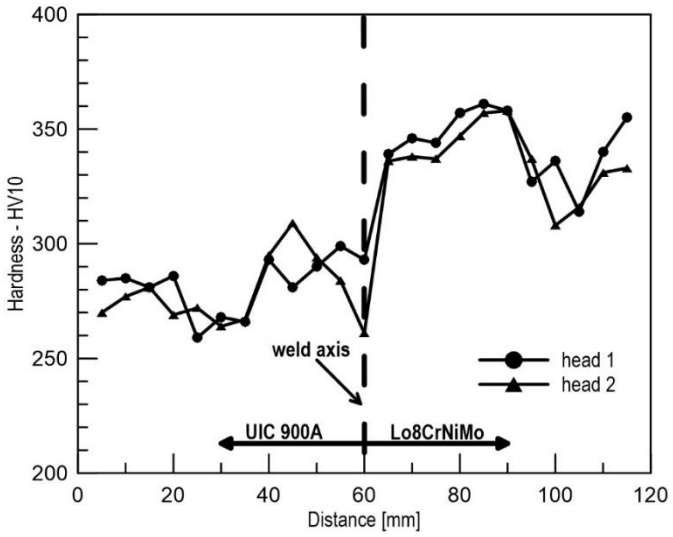

a) the head part of the weld

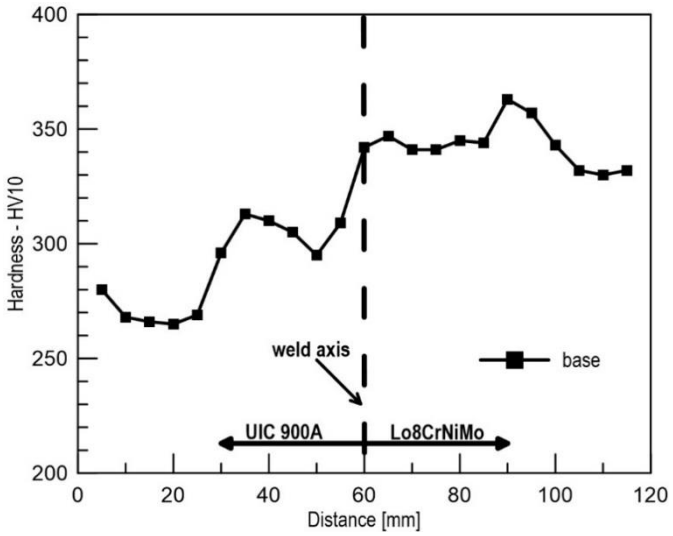

b) the base part of the weld

Fig. 2. Hardness behaviour, HV10.

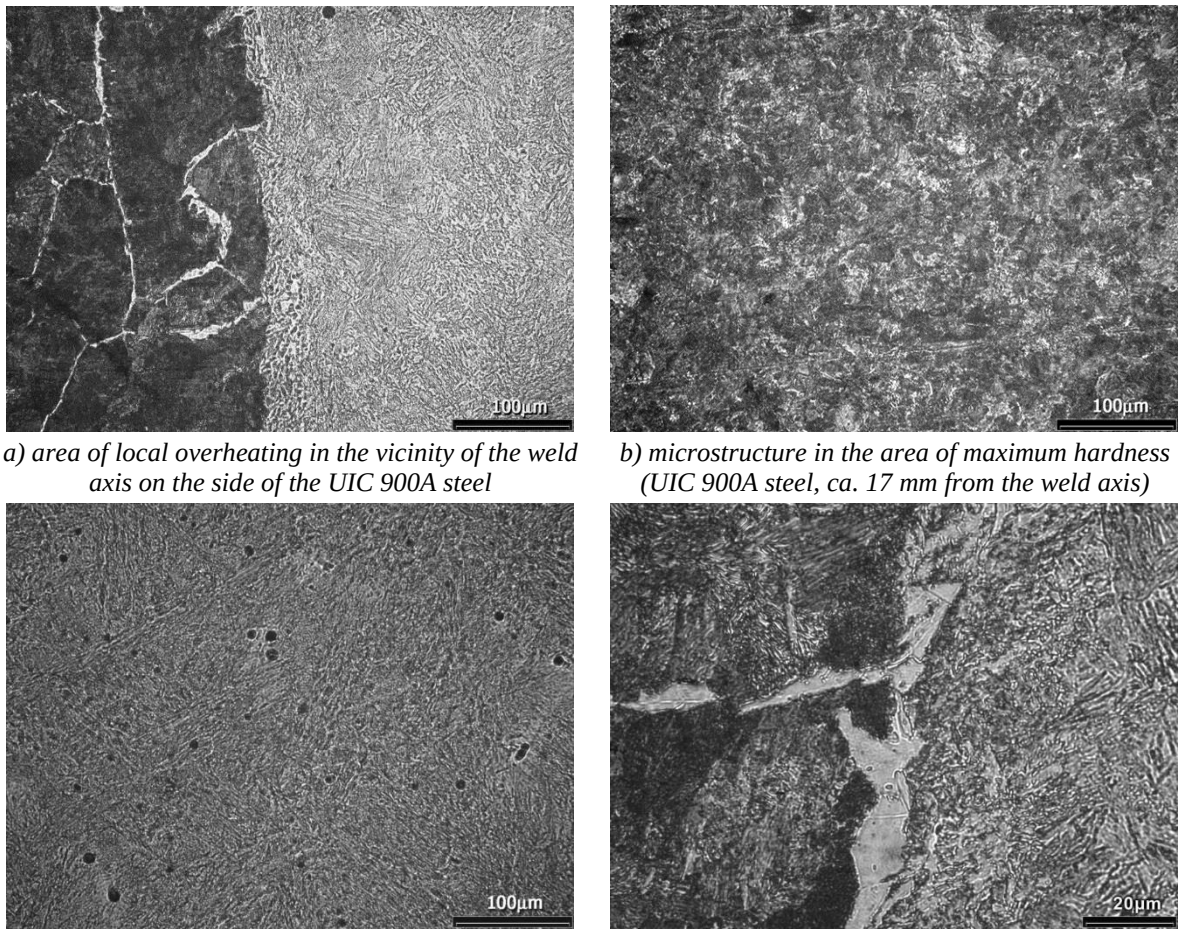

a) area of local overheating in the vicinity of the weld axis on the side of the UIC 900A steel

b) microstructure in the area of maximum hardness (UIC 900A steel, ca. 17 mm from the weld axis)

c) microstructure in the area of maximum hardness (Lo8CrNiMo steel, ca. 24 mm from the weld axis)

d) weld joint, the interface between UIC 900A–Lo8CrNiMo steels in the head part of the plate

Fig. 3. Microstructures observed in the location of the UIC 900A–Lo8CrNiMo steels weld joint (Nital).

Fig. 3c). The structure probably consisted of a mixture of upper and lower bainite.

The weld joint itself is formed by the thin melted layer. Segregated ferrite was observed at the interface between UIC 900A - Lo8CrNiMo steels in the head part of the plate (Fig. 3d). The probable cause was the redistribution of carbon between UIC 900A eutectoid steel and the low-carbon alloy steel Lo8CrNiMo. In the base part of the plate, a similar phenomenon was not observed.

3.2 The fracture behaviour

The following values of dynamic fracture toughness were evaluated:

- K_{Cd} - dynamic linear-elastic fracture toughness for tests terminated by cleavage. Calculated K_{Cd} values fail to fulfil the conditions given in the ASTM standard [11] although the force–displacement record was mainly linear up to fracture;
- K_{JCd} - the dynamic elastic-plastic fracture toughness converted from the J_{Id}-integral calculated by using the equation (1):

$$(J_I)_{init} = \frac{(K_I)^2_{init}(1-\nu^2)}{E} + \frac{2(A_{pl})_{init}}{B(W-a)} \qquad (1)$$

where $(K_I)_{init}$ is the elastic stress intensity factor for the initiation force F_{init} and $(A_{pl})_{init}$ is the plastic area (energy) under the force-displacement record to the force F_{init}. To convert $(J_I)_{init}$ to $(K_I)_{init}$, the relation (2):

$$(K_J)_{init} = \left[\frac{(J_I)_{init}\,E}{(1-\nu^2)}\right]^{1/2} \qquad (2)$$

was used. K_{JCd} values were calculated for the fracture force F_{FRd} of the tests terminated by cleavage fracture with no prior ductile tearing. The possibility of using Eq. (1) to calculate the J_{Id}-integral was checked, for example, in [9, 12];

- K_{Jud} - post-ductile tearing cleavage dynamic fracture toughness for test terminated by cleavage;
- K_{Jmd} - dynamic fracture toughness values at maximum load F_{max} for stable fracture behaviour and nonlinear test records.

The fracture toughness values obtained in low blow impact tests and the graphical representation of their temperature dependences are presented in Figs. 4 and 5. The curve of the form (3)

$$\left(K_{Cd};\, K_{JCd}\right)_{mean} = K_{min} + A\exp(BT) \qquad (3)$$

was fitted to the experimental data. Having chosen K_{min} = 20 MPa·m$^{1/2}$, the parameters A and B may be calculated by linear regression analysis. After determining the standard deviation, the one-sided tolerance bound calculated with confidence P = 0.95 can be established. Both curves are drawn in Figs. 4 and 5. It should be noted that the curves in Figs. 4 and 5 represent only the variation of the dynamic fracture toughness in the transition and lower shelf regions.

A) The fracture behaviour of base materials and their heat-affected versions

The temperature dependence of the dynamic fracture toughness of the standard rail steel UIC 900A is shown in Fig. 4a along with the temperature dependence of the dynamic fracture toughness of the same steel in the HAZ (17 mm from the weld axis). The fracture toughness values K_{Cd} in the HAZ are about the same as or slightly higher than the fracture toughness values of the base material.

A similar temperature dependence for the bainitic cast steel Lo8CrNiMo is presented in Fig. 4b along with the temperature dependence of the dynamic fracture toughness in the HAZ (24 mm from the weld axis). The values obtained correspond to the dynamic fracture toughness level previously observed for this steel [5, 6]. The Lo8CrNiMo steel shows a significant shift of dynamic fracture toughness towards higher values and lower temperatures in comparison with the standard rail steel. The shift of the heat-affected version of Lo8CrNiMo steel towards higher dynamic fracture toughness values in comparison with the base material is more substantial than in the case of UIC 900A steel. The dynamic fracture toughness values measured at –20 °C even correspond to the upper shelf value of dynamic fracture toughness.

B) The fracture behaviour of the weld

The temperature dependence of the individual values of dynamic fracture toughness in the weld joint axis area is plotted in Fig. 5a.

Through the experimental data, a curve of the form given by Eq. (3) was fitted along with the one-sided tolerance bound. The figure also contains the waveforms of the fracture toughness of both base metals and their heat-affected versions.

The fracture toughness values exhibit considerable scatter throughout the test temperature range (-60 to +60 °C). The primary cause of this phenomenon may be the heterogeneity of the weld joint, as a result of which the heads of the cracks can appear in very different structures with vastly different resistances to brittle fracture. An important role is also played by the non-planarity of the melting area, which together with the very small thickness of this area could lead to a different location of fatigue cracks in various test specimens. Although on the surface of the test plate the crack tip was located at the weld axis, in the middle of the plate it could be located in the pearlitic or bainitic part of the weld. The dynamic fracture

toughness values of the weld joint are located in a strip bounded by HAZ values of both base materials. At lower temperatures, the fracture behaviour approaches that of Lo8CrNiMo steel, while at higher temperatures it approaches that of UIC 900A steel. In order to characterize the unique behaviour of the weld, it is necessary to perform additional experiments with respect to the variation of the dynamic fracture toughness.

The experimental data representing the strength properties (hardness HV10) and fracture properties (dynamic fracture toughness) obtained at room temperature are summarized in Fig. 5b. The fracture behaviour of Lo8CrNiMo steel reaches the upper shelf value at this temperature. A significant finding resulting from this graph is that the lower limit of the toughness scatter band of the weld joint is situated above the scatter band of UIC 900A steel and its HAZ. In terms of resistance to brittle fracture initiation, it can be stated that the UIC 900A–Lo8CrNiMo weld does not reduce the fracture properties of the base materials.

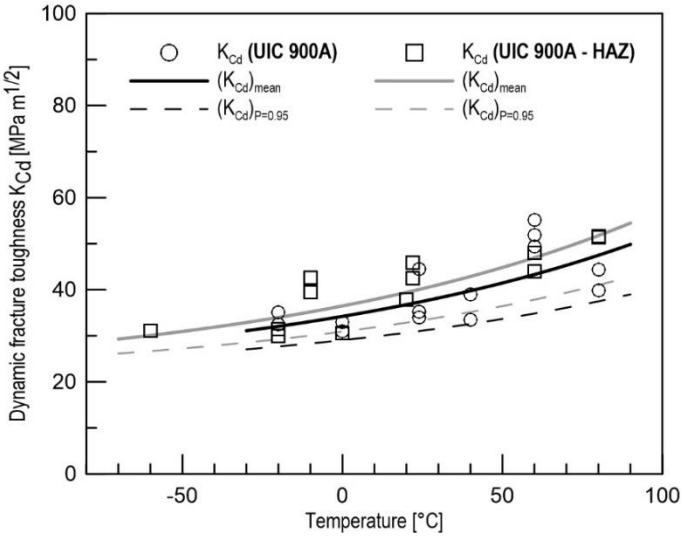

a) pearlitic (UIC 900A) steel

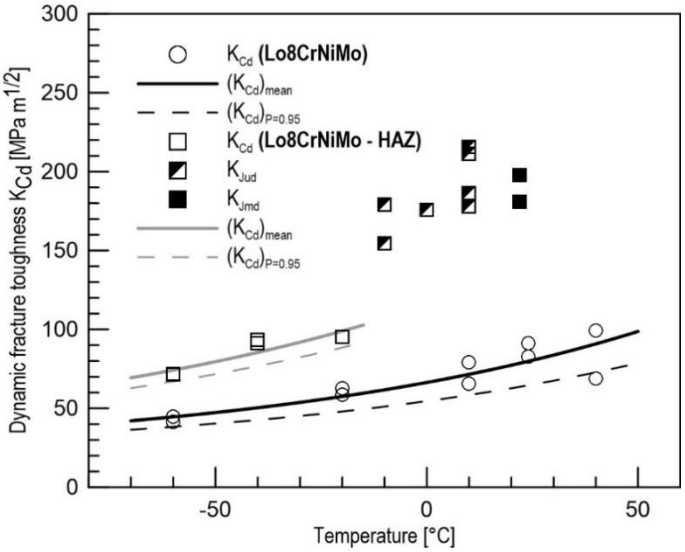

b) bainitic (Lo8CrNiMo) steel

Fig. 4. Dynamic fracture toughness comparison of HAZ and base material.

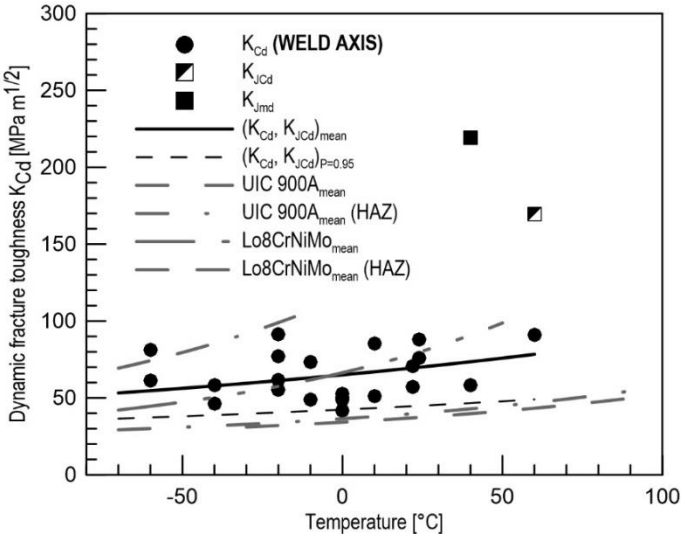

a) the temperature dependence of dynamic fracture toughness in the weld joint axis area

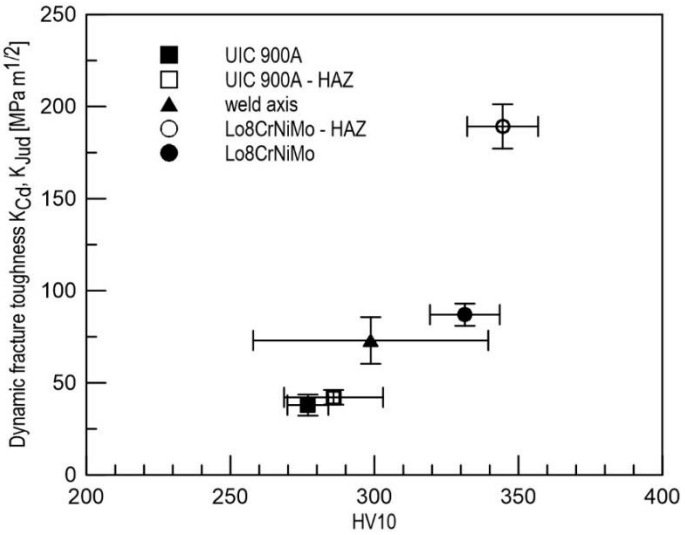

b) dependence of strength and fracture properties of the weld joint

Fig. 5. The fracture behaviour of the weld.

4. Conclusions

The microstructure and hardness and fracture behaviours of bainitic Lo8CrNiMo and standard rail UIC 900A steels intended for the production of railway frogs have been evaluated in the article.

The maximum hardness values measured in the heat affected zone (HAZ) of UIC 900A steel are between 29 and 33.5 HRC, while those in the HAZ of Lo8CrNiMo steel are between 37 and 39 HRC. The hardness values in the HAZ are not significantly different from those of the base materials. In the head part of the rail, the distance between the weld axis and the point of maximum hardness was about 24 mm in the case of bainitic steel, while in the case of UIC 900A steel it was ca. 17 mm. The structure of the weld joint on the side of UIC 900A rail steel consists of coarse pearlitic structure with ferrite excluded at the grain boundaries (with Widmanstätten pattern in some cases). Coarse-grained bainitic structure was found on the side of Lo8CrNiMo steel and changed very quickly into the tempered bainitic structure.

In the temperature range from –60 to 80 °C, the fracture toughness of UIC 900A steel is located in the lower shelf region of fracture toughness, where only a weak temperature dependence of fracture toughness

can be found. The temperature dependence of K_{Cd} in the HAZ of UIC 900A steel is basically comparable with the temperature dependence of the K_{Cd} of the base material and is only slightly shifted to lower temperatures and higher fracture toughness values. From this it follows that the resistance to brittle fracture initiation does not deteriorate significantly in this area.

In the temperature range from -60 to 40 °C, the dynamic fracture toughness values of the base material Lo8CrNiMo inhere in the transition region of the temperature dependence of the fracture toughness. The dynamic fracture toughness values of the Lo8CrNiMo steel in the HAZ cover the complete ductile-to-brittle transition in the temperature range of -60 to 22 °C, whereas the fractures were initiated by ductile micromechanism at temperatures above –10 °C. That means that the resistance to brittle fracture increases considerably in the HAZ of the Lo8CrNiMo steel.

Throughout the test temperature range (-60 to +60 °C), the fracture toughness values of the specimens taken from the weld axis exhibit substantial scatter. This effect is probably caused by the heterogeneity and non-planarity of the weld joint, and thus the fatigue crack positions of particular test specimens are in different positions relative to the weld location. The dynamic fracture toughness values of the weld joint are located in a band that is upper bounded by the HAZ values of Lo8CrNiMo steel and lower bounded by the HAZ values of UIC 900A steel.

It can be stated that the weld joint of Lo8CrNiMo and UIC 900A steels does not negatively affect the fracture properties of the base materials.

Acknowledgements

The works have been supported by the project NETME centre plus (Lo1202), project of Ministry of Education, Youth and Sports of the Czech Republic under the "national sustainability programme".

References

[1] E. Karczmarczyk, T. Kufa, P. Matušek: Hutnické listy 7-8 (1994) 34-42.

[2] D. Davis, M. Scholl, H. Sehitoglu: Railway, Track and Structures (1997) 14-16.

[3] U.P. Singh, B. Roy, S. Bhattacharyya, S.K. Jha: Mater. Sci. Tech. 17(1) (2001) 33-38.

[4] E. Schmidová: Zvyšování užitných vlastností kolejnicového materiálu *(Enhancement of utility properties of the rail material)* (dissertation thesis), BUT 2002. *(in Czech)*

[5] J. Zbořil: In: Vědeckotechnický sborník českých drah 11, Praha 2001, pp. 63-79.

[6] M. Holzmann, I. Dlouhý, J. Zbořil: Hutnické listy 57 (2003) 8-20.

[7] B. Zlámal: Hodnocení svarů bainitické oceli na odlitky *(Evaluation of cast bainitic steel welds)* (diploma thesis), BUT 2003. *(in Czech)*

[8] ASTM E23.03.03 Proposed standard method of tests for instrumented impact testing of precracked Charpy Specimens of metallic materials, Revised dynamic fracture toughness test methods, Draft 12, September 2000.

[9] J. Man, M. Holzmann, B. Vlach: Zváranie 36 (1987), 291-294 (part I), 323-327 (part II), 355-356 (part III). (*in Czech*)

[10] ČSN 42 0462 Zkoušení kovů. Stanovení velikosti zrna ocelí a neželezných kovů *(Metal testing. Methods for estimating the average grain size of steel and non-ferrous metals)* 2014. *(in Czech)*

[11] ASTM E 399 Standard test method for plain-strain fracture toughness of metallic materials 2012.

[12] W.L. Server: J. Test. Eval. 6(1) (1978) 29-34.